N. H. Yang,[1] *H. Nayeb-Hashemi,*[1] *and A. Vaziri*[2]

Multi-Axial Failure Models for Fiber-Reinforced Composites

ABSTRACT: Combined in-phase tension/torsion loading was applied to 8-ply $[\pm 45°]_4$ E-glass/epoxy composite shafts under monotonic and fatigue conditions to determine the effects of multi-axial loading on its failure. A damage criterion for multi-axial monotonic loading was proposed considering the contribution of both normal and shear stresses on the plane of failure. The experimental data showed an excellent agreement with the proposed model for various loading conditions. Several multi-axial fatigue failure models were proposed considering mean and cyclic normal stress and shear stress at the plane of failure, as well as the mean and cyclic normal strain and shear strain at the plane of failure and their capability for predicting the fatigue life of the composite under study was examined. In addition to the fatigue damage model based on the plane of failure, a multi-axial fatigue failure model was proposed considering the mean and cyclic energy in the fatigue experiments. The experimental data showed a reasonably good correlation with some of the proposed damage models.

KEYWORDS: multi-axial loading, fiber-reinforced composites, fatigue failure, monotonic failure

Introduction

Fiber-reinforced composites are extensively used in manufacturing of various components in engineering structures such as high-pressure vessels, aerospace structures, transmission shafts in automobiles, support structures, etc. Traditional materials are being replaced by composites due to their high strength to weight ratio, corrosion resistance, and cost. The increasing use of composite structures has highlighted the need for models to determine the monotonic and fatigue characteristics of composites under multi-axial stress fields. Many multi-axial fatigue damage models based on strain, stress, and energy data have been proposed in an attempt to correlate the data with fatigue life. However, a general theory capable of modeling the fatigue life of a variety of materials subject to different loading conditions is not available. Studying previously proposed multi-axial failure models, in conjunction with an understanding of the damage mechanism and failure modes can help immensely in developing multi-axial failure models for fiber-reinforced composites. An overview of damage mechanisms and failure modes of fiber-reinforced composites under multi-axial loading is provided in the next section. Moreover, previously proposed multi-axial failure models for both isotopic and anisotropic materials are discussed briefly.

Failure Mechanisms of Fiber-Reinforced Composites Under Multi-Axial Loading

Fiber-reinforced composites fail due to accumulation of damage rather than from the growth of a single crack. The different damage mechanisms which occur during loading include fiber/matrix debonding, matrix cracking, delamination, fiber fracture, etc. Kaynak and Mat [1] performed uniaxial fatigue tests on $[\pm 55°]$ glass/epoxy composite tubes. They evaluated the effect of stress level and especially loading frequency on the different stages of failure as (1) matrix crazing, (2) fiber/matrix debonding and delamination, and (3) fiber fracture.

Krempl and Niu [2] studied the failure of graphite/epoxy $[\pm 45°]$ tubes under static and fatigue loadings. In static loading, failure was initiated by delamination of the outer layer for both tensile and compressive loadings. Combined in-phase cyclic loading under load control was used to study the influ-

---

[1] Graduate Research Assistant and Professor of Mechanical Engineering, respectively, Northeastern University, Boston, MA 02115.

[2] Lecturer on Engineering and Research Associate, Division of Engineering and Applied Sciences, Harvard University, Cambridge, MA 02138.

ence of combined loading on fatigue life. Failure initiation was characterized by fiber fractures, splitting of the laminates parallel to fibers and some debonding between adjacent layers of the laminates.

Fleck and Jelf [3] performed compression-torsion tests on pultruded carbon/epoxy tubes. They listed six failure mechanisms of fiber composites due to compressive loads: (1) matrix failure, (2) fiber crushing, (3) splitting from one end of the specimen, (4) surface delamination driven by elastic buckling of a surface-debonded layer, (5) elastic buckling, and (6) plastic micro-buckling. Radon and Wachnicki [4] studied the fatigue crack growth in a chopped strand mat of glass fiber reinforced polyester resin under biaxial loading. The fatigue crack growth rate was evaluated through the changes in the specimen compliance. It was shown that the fatigue crack growth in this material could be governed by a Paris law relationship as

$$da/dN = C(\Delta K)^m \tag{1}$$

where N is the number of cycles, a is the crack length, C and m are material constants, and ΔK is the alternating stress intensity factor which is a function of the gross stress, finite width correction factor and the normalized crack length. The micro-mechanisms of the crack growth were based on accumulation of various damage modes such as fiber breakage, matrix crazing, and layer debonding.

Failure of fiber-reinforced composite is a complex process due to the possible contribution of multiple damage mechanisms. Failure can initiate at multiple locations and is dependent on the local stress field in the composite. The intricate nature of the failure in fiber-reinforced composites, which is indeed governed by highly complex interacting mechanisms, makes development of a failure model for these materials a challenging task. An understanding of the damage mechanisms which lead to the final failure of the fiber-reinforced composites under multi-axial loading is essential in developing failure models for fiber-reinforced composites.

Multi-Axial Failure Models for Isotropic Material

Under cyclic loading, metals and metal alloys differ from composites in that metals tend to fail with the growth of a single crack, whereas composites generally fail due to accumulation of various damages. Metals also exhibit flow and hardening factors that must be accounted for in fatigue models. However, the methods proposed to predict fatigue failure in metals may provide insights to developing damage criteria and fatigue life prediction of fiber-reinforced composites.

There are three commonly used methods to predict multi-axial fatigue failure in isotropic material: effective stress-strain method, work/energy method, and critical plane of failure method. The effective stress-strain method reduces a three-dimensional stress state to an effective stress state parameter. Two examples are the Von Mises Failure Criterion and the Tresca Failure Criterion. The Von Mises Criterion relates the total number of cycles to failure with an effective stress parameter. The Tresca Criterion relates the total number of cycles to failure with the maximum shear stress. Leese and Morrow [5] proposed a fatigue failure model from torsional low cycle fatigue tests on thin-walled steel tubular specimens using the effective shear strain approach. Assuming that the total shear strain is the summation of the elastic and plastic shear strains when the material is subjected to pure shear, the fatigue life N_f was related to the total shear strain as

$$\frac{\Delta \gamma}{2} = \frac{\tau'_f}{G}(2N_f)^{b_o} + \gamma'_f(2N_f)^{c_o} \tag{2}$$

where τ'_f is the torsional fatigue strength coefficient, γ'_f is the torsional fatigue ductility constant, N_f is the number of cycles to failure, G is the shear modulus, and b_o and c_o are material constants. Fash et al. [6] performed multi-axial fatigue experiments to examine the validity of the effective strain method for predicting fatigue life of hot-rolled steel. The effective strain model was expressed as

$$\frac{\Delta \bar{\varepsilon}}{2} = \frac{\sigma'_f}{E}(2N_f)^b + \varepsilon'_f(2N_f)^c \tag{3}$$

where σ'_f is the fatigue strength coefficient, ε'_f is the fatigue ductility coefficient, E is Young's modulus, b and c are material coefficients, and $\bar{\varepsilon}$ is the effective strain parameter defined as

$$\bar{\varepsilon} = \frac{\sqrt{2}}{3}[(\varepsilon_1 - \varepsilon_2)^2 + (\varepsilon_2 - \varepsilon_3)^2 + (\varepsilon_1 - \varepsilon_3)^2]^{\frac{1}{2}} \tag{4}$$

where ε_1, ε_2, and ε_3 are the strain in the principal directions.

The work/energy method relates the fatigue life to the amount of energy needed to cause failure. Ellyin et al. [7–13] have studied the multi-axial fatigue damage of a variety of metal alloys and proposed a multi-axial fatigue failure model based on the strain energy density damage law. A fatigue failure criterion was proposed relating the total strain energy density, ΔW^t, to the number of cycles to failure N_f as

$$\Delta W^t = \kappa N_f^\alpha + C \tag{5}$$

where κ, α, and C are material constants estimated from experimental data.

Ellyin and Kujawski [13] proposed an alternative damage criterion considering the effects of mean stress on the cyclic plastic strain energy as

$$\psi = \frac{\Delta W_d h(\sigma_m)}{f(\bar{\rho})} \tag{6}$$

where ΔW_d is the distortion strain energy range, $f(\bar{\rho})$ is a function of the multi-axial constraint, and $h(\sigma_m)$ is a function of the tensile mean stress.

The critical plane method utilizes the normal and shear stresses and strains at the plane of failure as damage parameters in the failure model. Two cases are considered [14]; for Case A, the critical plane of failure is defined as the one that crack propagates along the surface of the specimen, and for Case B, the crack grows away from the surface and into the specimen. Based on these two planes, the fatigue damage parameter is defined as

$$\gamma^* + k\varepsilon^* = f(N_f) \tag{7}$$

where k is a constant, γ^* is the shear strain amplitude, and ε^* is the normal strain amplitude to the critical plane. Socie et al. [15] modified the above equation based on multi-axial fatigue tests on Inconel 718. The fatigue damage model was defined as:

$$\gamma_p^* + k\varepsilon_{np}^* = f(N_f) \tag{8}$$

where γ_p^* and ε_{np}^* are the plastic shear strain amplitude and the plastic strain amplitude normal to the critical plane for growth of the crack into the specimen, respectively. The above models do not consider the effect of the mean stress and strain at the critical plane of failure. Socie et al. [15] modified these damage models by incorporating the effect of normal mean stress at the critical plane into the damage model as

$$\gamma_p^* + k\varepsilon_{np}^* + \frac{\sigma_{no}^*}{E} = f(N_f) \tag{9}$$

where σ_{no}^* is the mean normal stress at the critical plane and E is the material Young's modulus.

Stephens et al. [16] proposed a fatigue damage parameter based on the maximum shear strain at the critical plane, γ_{max} and the maximum normal stress at the critical plane, σ_n^{max}, as

$$\gamma_{max}\left(1 + \frac{n\sigma_n^{max}}{\sigma_y}\right) = f(N_f) \tag{10}$$

where σ_y is the material yield strength and n is a constant.

The Smith, Watson and Topper (SWT) model [17] identifies a plane of failure and relates the fatigue life to the maximum normal stress and the cyclic strain on the plane of failure as

$$\sigma_1^{max}\frac{\Delta\varepsilon_1}{2} = f(N_f) \tag{11}$$

where σ_1^{max} is the maximum normal stress and $\Delta\varepsilon_1$ is the cyclic strain.

Multi-Axial Failure Models for Anisotropic Material

There is relatively little literature on the effect of multi-axial loading on the fatigue life of anisotropic materials. A study recently performed at the Marshall Space Center [18] produced a temperature and time dependent mathematical model to predict the conditions for failure of a material subjected to multi-axial loads. The model was applied to a filled epoxy below its glass-transition temperature and is applicable for temperatures in the range of -20 and $115°F$. This model is in the form of

$$AP^2 J_2 + BPI_1 = 1 \qquad (12)$$

where J_2 is the second deviatoric, I_1 is the first stress invariant, and A, B, and P are temperature dependent parameters which define the shape of the failure surface in the multi-axial stress space. Although this model is for static loading, the damage model can be compared to experimental results to determine if there is a correlation between the number of cycles to failure and the proposed multi-axial damage model.

Found [19] proposed a conservative failure criterion for chopped fiber-reinforced composites, woven fabric-reinforced composites and fabric-reinforced composites under biaxial static and fatigue loading conditions. He suggested a conservative estimate for design purposes where the failure in the tension/tension quadrant is given by a circular arc and by a straight line in the tension/compression quadrant. The proposed failure models were given as

$$\left(\frac{\sigma_1}{F_{1t}}\right)^2 + \left(\frac{\sigma_2}{F_{2t}}\right)^2 = 1 \qquad (13)$$

$$\left(\frac{\sigma_1}{F_{1t}}\right) - \left(\frac{\sigma_2}{F_{2c}}\right) = 1 \qquad (14)$$

where σ_1 and σ_2 represent stresses in the principal directions, F_{1t} and F_{2t} are the tensile strengths in the principal directions, and F_{2c} is the compressive strength in the principal direction.

Caprino [20] developed a model to predict the fatigue life of randomly oriented glass fiber-reinforced plastics under tension-tension fatigue and applied it to experimental data available in the literature. The proposed model is in the form of,

$$N = \left[1 + \frac{1}{\alpha(1-R)}\left(\frac{\sigma_o}{\sigma_{max}} - 1\right) \right]^{1/\beta} \qquad (15)$$

where α and β are constants, R is the stress ratio ($\sigma_{min}/\sigma_{max}$), σ_o is the monotonic strength of the virgin material, and σ_{max} is the maximum stress during cyclic loading. Although this model is for uniaxial loading, the method could be used to predict multi-axial fatigue failure in anisotropic materials.

Hashemi et al. [21,22] performed multi-axial fatigue experiments on textured 6061-T6 aluminum rods. Experiments were carried out at room temperature under three types of loading conditions: tension-compression, torsion, and combined tension-torsion. An anisotropic multi-axial failure model was proposed as

$$\gamma_{max} + B_i \varepsilon_n = f(N_f) \qquad (16)$$

where γ_{max} and ε_n denote the maximum shear and the normal strain on the plane of failure, respectively, and B_i is a material constant.

Van Paepegem and Degrieck [23–26] and Van Paepegem et al. [27] provided a review of the existing models for fiber-reinforced composites. Moreover, they proposed a residual stiffness model that predicts the stiffness degradation and final failure of the composite based on the static Tsai-Wu failure criterion. The proposed model, validated by finite element simulations, was capable of predicting the stress distributions, stress-cycle history, and damage distributions in bending fatigue experiments of plain woven glass/epoxy composites.

Energy method has also been employed in predicting the fatigue behavior of fiber-reinforced composites. Shokrieh and Taheri-Behrooz [28] proposed a fatigue life model based on the energy method for unidirectional polymer composite laminates under tension-tension and compression-compression fatigue loading. Natarajan et al. [29] proposed a fatigue model based on strain energy density by performing

TABLE 1—*Mechanical properties of the E-glass/epoxy individual lamina.*

E_1	E_2	G_{12}	ν_{12}	Thickness
53.0 GPa	17.65 GPa	8.82 GPa	0.25	0.158 mm

tension-tension and bending fatigue experiments on fiber-reinforced polymeric composites. Although both methods predicted the fatigue life of their respective specimens reasonably well, they did not investigate the influence of combined loadings such as tension-torsion fatigue.

Based on the literature survey, there are not extensive studies on the development of a multi-axial fatigue failure model for fiber-reinforced composites. In this study, the failure characteristics of E-glass/epoxy $[\pm45°]_4$ tubes under combined tension-torsion loading are studied and various damage model criteria for composite laminates under multi-axial loadings are proposed and their capability for predicting the failure of the composite is examined. The main objective of this work is to develop a damage criterion that can be used for multi-axial fatigue life prediction. Similar to many other engineering structures, the composite under investigation has anisotropic properties which must be accounted for in the damage criteria. New fatigue models for predicting the multi-axial fatigue life of fiber-reinforced composites are proposed by extending the three methods previously developed for isotropic materials.

Experimental Investigation

Material

The material used in this investigation was E-glass/epoxy composite with fiber volume fraction of 55 %. The material was provided in the form of a prepreg by Aldila, Inc. The mechanical properties of the individual lamina were obtained using the ultrasonic method [30] and are shown in Table 1.

The composite specimens were manufactured by wrapping eight layers of prepreg around an aluminum mandrill with fiber direction alternating at ±45° in respect to the vertical axis. Prior to manufacturing, the mandrill was cleaned with XTEND CX-500 mold cleaner and then coated with XTEND SAM-19 mold release (supplied by AXEL Plastics) to ensure easy release of the composite tubes. A six-in. wide, thin aluminum sheet was wrapped around the composite layers and then shrink wrap tape provided by Dunstone Company, Inc. was wrapped around the entire specimen before it was cured at 180°C for 90 min. The mandrill was removed once the specimen returned to room temperature. The product of the process was a $[\pm45°]_4$ E-glass/epoxy composite tube with an inner diameter of 25.4 mm and an outer diameter of 27.94 mm and approximately 304.8 mm long.

Two dumbbell shape inserts were used to make the overall dog bone shape specimen (Fig. 1). To ensure alignment of the inserts with the specimen axis, a rod was passed though the center of the entire assembly. Furthermore, an aluminum insert with the length of 50.8 mm was inserted between the two dumbbells. The aluminum insert produced nearly zero gap at its interface with the dumbbell inserts and was free and was not carrying any load during the experiments. However, it prevented micro-buckling in the composite tube during torsion tests and maintained the tube diameter during tensile tests, thus exerting an internal pressure on the composite tube. The composite tube was glued to the dumbbells using ECCOBONDG-909 and was cured at 180°C for 60 min. The alignment rod was removed from the assembly prior to the experiment.

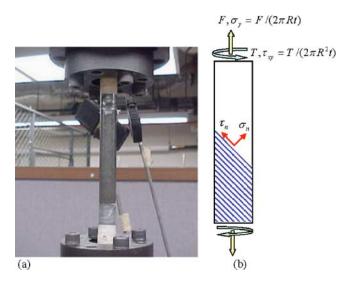FIG. 1—*Composite/dumbbell assembly test specimen.*

FIG. 2—(a) Composite specimen in the Instron machine prior to tension/torsion experiments. (b) Schematic figure of the composite specimen with average radius, R, and thickness t, subjected to monotonic multi-axial loading. The outer layer fibers are shown schematically. σ_n and τ_n are the normal and shear stresses on the plane 45° to the specimen axis (transverse to fiber direction) used in developing the failure models for the composite.

Multi-Axial Loading

An Instron 1322 tension/torsion machine was used to apply multi-axial loads to the composite shafts (Fig. 2(a)). All monotonic tests were carried out under load control with tensile and torsional loading rates less than 450 N/s and 740 N.mm/s, respectively. Experiments with different ratios of the maximum tensile load to the maximum torsional load (50, 25, 10, 5, 0 %) were carried out. A total of 30 specimens were tested at various combinations of tension loading and torsion loading. The experiments were stopped after total failure of the composite shafts.

All fatigue tests were performed under load control at frequency of 1 Hz. Specimens were subjected to one of three different multi-axial loading conditions. Figure 2(b) shows the schematic of the composite specimen subjected to multi-axial tension/torsion loading. The applied average tensile and shear stress in the composite are related to the applied far field tensile and torsion loadings using basic equilibrium equations. The first multi-axial fatigue experiment was performed with cyclic tension at a mean tensile stress and fully reversible torsion. The mean tensile stress for all experiments was 119 MPa. The second multi-axial loading condition was a constant torsion and cyclically applied tension at a mean tensile stress. The final multi-axial loading condition was a constant tensile load with full reversible cyclic torsion. The experiments were stopped when the composite specimens failed. Data were recorded in real-time mode on four channels: axial force, axial displacement, torsion force, and angular displacement by a computer software program.

Results and Discussion

Damage Mechanisms Due to Multi-Axial Loading

During multi-axial loading, damage was observed as white lines forming along the fiber/matrix interface of the composite shafts indicating possible craze formation in the matrix and fiber/matrix debonding (Fig. 3). Regions of delamination were also observed within the composite. This is consistent with observation made in Ref. [1]. Micro-cracks in the fiber free zones accumulate and weaken the fiber/matrix interface. Audible failure could be heard in the late stages of the experiments. These audible damage mechanisms were attributed to delamination and fiber fracture.

Figure 3 shows the growth and accumulation of damage within the composite. There are a number of locations where final failure of the composite may initiate. However, it was observed during the experiment that final failure initiated in the outer layer at 45° to the specimen axis. This can be justified by
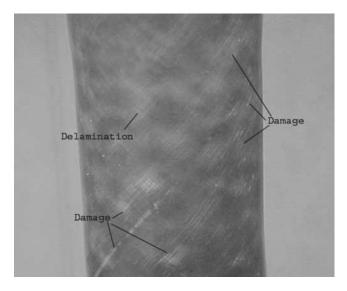
FIG. 3—*Damage mechanisms of composite shaft subjected to multi-axial loading. Damage propagation can be seen along the fiber direction at 45°. Light colored region indicates delamination in the composite.*

considering the local stress field at the fiber/matrix interface. After fiber/matrix debonding occurs, the local stress field becomes very complex and the normal and shear stresses will cause delamination of subsequent layers. The growth of damage at the 45° fiber/matrix interface causes a weakened area where failure is initiated. Final failure occurred at the fiber/matrix interface with the greatest accumulation of damage.

Monotonic Failure Model

Figure 4 shows the failure locus of the composite shafts due to multi-axial loading. The quadratic failure criterion leads to an acceptable fit to the experimental data. However, a closer examination of failed specimens indicated that the failure in a majority of the specimens initiated at the outer lamina in the 45° plane to the specimen axis (Fig. 5). The damage mode suggests that a combination of shear stress and normal stress on the plane of failure may be responsible for the failure of the composite shafts. Using the classical lamination theory, the strains at the mid-surface plane of the composite tube were calculated from the applied tension and torsion. The in-plane forces per unit length in the circumferential direction, N_y and N_{xy} were found as

$$N_y = \frac{F}{2\pi R} \tag{17}$$

$$N_{xy} = \frac{T}{2\pi R^2} \tag{18}$$

where F was the applied axial load and T was the applied torsion load. The strains in the mid-surface of the composite are found from the composite lamination theory as
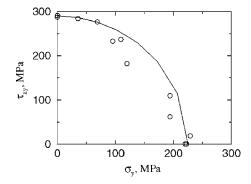

FIG. 4—*Monotonic failure locus based on applied axial stress and shear stress.*

FIG. 5—*Typical failure mode of a composite specimen from a monotonic multi-axial test.*

$$\begin{bmatrix} N_x \\ N_y \\ N_{xy} \end{bmatrix} = \begin{bmatrix} A_{11} & A_{12} & 0 \\ A_{21} & A_{22} & 0 \\ 0 & 0 & A_{66} \end{bmatrix} \begin{bmatrix} \varepsilon_x^o \\ \varepsilon_y^o \\ \gamma_{xy}^o \end{bmatrix} \tag{19}$$

$$A_{ij} = \sum_{k=1}^{N} (\bar{Q}_{ij})_k (z_k - z_{k-1}) \tag{20}$$

where the strain ε_x^o (hoop strain) is assumed to be zero, since the aluminum insert prevents radial displacement. The $[A]$ matrix represents the stiffness matrix of the composite laminate and $(\bar{Q}_{ij})$ is the component of the stiffness matrix of the individual lamina, which is obtained from the elastic properties of the composite in the material principal direction, and z_k is the location of the lamina in the composite. A MATLAB program was written to evaluate $\bar{Q}_{ij}$ and A_{ij} components. The normal and shear stresses in the 45° plane at the outer layer is subsequently obtained from

$$\begin{bmatrix} \sigma_x \\ \sigma_y \\ \tau_{xy} \end{bmatrix}_k = [\bar{Q}]_k \begin{bmatrix} \varepsilon_x^o \\ \varepsilon_y^o \\ \gamma_{xy}^o \end{bmatrix} \tag{21}$$

The stress field in the plane of failure is then obtained from the stress transformation as

$$\sigma_n = \frac{\sigma_x + \sigma_y}{2} + \frac{\sigma_x - \sigma_y}{2} \cos(2\phi) + \tau_{xy}\sin(2\phi) \tag{22}$$

$$\tau_n = -\frac{\sigma_x - \sigma_y}{2} \sin(2\phi) + \tau_{xy}\cos(2\phi) \tag{23}$$

Based on the assumption that a combination of the normal and shear stresses at the plane of failure are responsible for final failure, a multi-axial failure model for monotonic loading was proposed as

$$\sigma_n + \alpha\tau_n = C \tag{24}$$

where σ_n and τ_n are normal and shear stresses at the outer layer surface at the 45° plane from Eqs 22 and 23 and α and C are material constants. The material constants α and C were evaluated with a regression analysis and were found to be 2.9 and 509 MPa, respectively. Figure 6 shows the linear relationship between the normal stress and shear stress at the plane of failure required to cause failure during multi-axial monotonic loading. The results showed an excellent agreement between the experimental data and theoretical results.
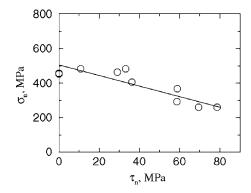
FIG. 6—*Failure criteria for multi-axial monotonic loading. Upon failure of the composite specimen, a linear relationship is observed between the normal and shear stresses at the plane of failure.*

Fatigue Failure Models

Fatigue failure of a majority of the specimens initiated again on the outer surface of the composite laminate at 45° to the specimen axis (Fig. 7). A damage model was proposed similar to the monotonic failure model proposed in Eq 24 by incorporating the role of the mean and cyclic stresses at the plane of failure. Using again the classical lamination theory, the stress field at the outer layer was evaluated to identify the mean and cyclic stresses at the plane of failure. A one parameter fatigue damage model incorporating both cyclic stress amplitudes and mean stresses was defined as

$$D = \frac{(\sigma_n)_a + \alpha(\tau_n)_a + (\sigma_n)_m + \alpha(\tau_n)_m}{C} \tag{25}$$

where $(\sigma_n)_a$ and $(\tau_n)_a$ denote the amplitude of the normal and shear stresses, respectively, $(\sigma_n)_m$ and $(\tau_n)_m$ denote the normal and shear mean stresses, respectively, α is a material constant which was evaluated to be 2.29 for the composite under study, and C is the magnitude of the monotonic failure strength defined in Eq 24 and is equal to 138.07 MPa. The experimental data are somewhat scattered using this damage model (Fig. 8). The contribution of mean normal stress is more detrimental to the fatigue life of a composite than the mean shear stress, as the mean normal stress reduces the crack surface interaction. To account for this effect, different weighting factors were incorporated for the mean and shear normal stresses to develop a two-parameter fatigue damage model which is in the form of

$$D = \frac{(\sigma_n)_a + \alpha(\tau_n)_a + (\sigma_n)_m + \beta(\tau_n)_m}{C} \tag{26}$$

where α and β are material constants, obtained to be 2.35 and 1, respectively, for the composite under study. This model predicts fatigue life of the composite shafts under various loading conditions reasonably well (Fig. 9). To verify the above damage model, two other multi-axial loading conditions were investigated, cyclic tension under constant torsion and fully reversible cyclic torsion under a constant tensile load.

FIG. 7—*Typical failure mode of the composite tube in a multi-axial fatigue experiment, showing failure is in the 45° plane to the specimen axis.*
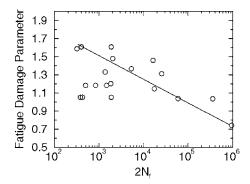
FIG. 8—*Damage parameter (Eq 25) versus fatigue life of composite tube for cyclic tension/torsion multi-axial fatigue experiments.*

In order to account for various multi-axial loading conditions, Eq 26 was modified by incorporating two additional material constants, A and B,

$$D = \frac{A(\sigma_n + \alpha\tau_n)_a + B(\sigma_n + \beta\tau_n)_m}{C} \tag{27}$$

The value of A and B for the composite under study is evaluated to be 0.267 and -0.00264, respectively. This model predicts fatigue life reasonably well for various multi-axial loading conditions (Fig. 10).

We have also considered a damage model based on the magnitude of cyclic and mean energies. This energy damage model is similar to the failure model proposed by Ellyin et al. [8] and is in the form of
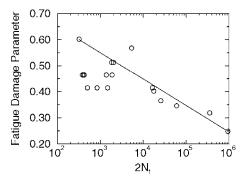

FIG. 9—*Modified damage parameter (Eq 26) versus fatigue life of composite tube for cyclic tension/torsion multi-axial fatigue experiments, indicating a better correlation compared to the model proposed in Eq 25.*
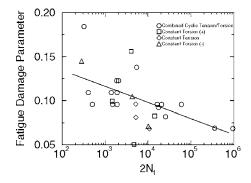

FIG. 10—*Modified damage parameter (Eq 27) versus fatigue life for various multi-axial fatigue experiments, revised to account for constant torsion and cyclic tension.*
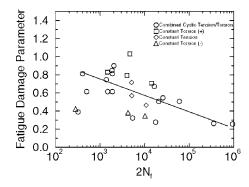
FIG. 11—*Energy damage parameter (Eq 28) versus fatigue life for various multi-axial fatigue experiments.*

$$D = \frac{1}{2}\alpha(\sigma_x\varepsilon_x + \sigma_y\varepsilon_y + \tau_{xy}\gamma_{xy})_{mean} + \frac{1}{2}\beta(\sigma_x\varepsilon_x + \sigma_y\varepsilon_y + \tau_{xy}\gamma_{xy})_{amplitude} \tag{28}$$

where σ_x, σ_y, and τ_{xy} are the average stress in the laminate, ε_x, ε_y, and γ_{xy} are the mid-plane strains and α and β are material constants, evaluated as 1.28 and 1.09, respectively, for the composite under study. Figure 11 shows a slight scatter of the experimental data and the prediction from Eq 28.

As a finalized step, a damage model was proposed considering the cyclic normal and shear strains rather than stresses at the plane of failure. This damage model is in the form of

$$D = \alpha(k\varepsilon_n + \gamma)_{mean} + \beta(k'\varepsilon_n + \gamma)_{amplitude} \tag{29}$$

where α, β, k, and k' are material constant (-10.0, 10.0, -0.0264, and 2.67, respectively for the composite under study) and ε_n and γ are the strains at the critical plane of failure. The strains at the plane of failure were found with a similar transformation used for the stresses in Eqs 22 and 23. This damage model predicts fatigue failure reasonably well for various loading conditions (Fig. 12).

Comparison of the experimental data with the multi-axial fatigue life models proposed here show the data are somewhat scattered compared to the monotonic model. This could be related to the loading frequency, the visco-elastic properties, and the complex nature of the fatigue failure in composite material. During the fatigue experiments, the temperature of the specimens increased which could affect the failure mechanisms of the composite. Moreover, a proper damage model should consider the influence of frequency and visco-elastic properties of composites.

Conclusions

Monotonic and fatigue experiments were performed to observe the effects of multi-axial loading on the strength properties of E-glass/epoxy composite shafts. Damage was observed to accumulate over the loading period as matrix cracking and crazing, fiber/matrix debonding, delamination, and fiber fracture. Final failure for monotonic and fatigue loading conditions initiated in the outer layer at 45° to the specimen axis. A multi-axial monotonic failure criterion was proposed considering the stresses at the plane
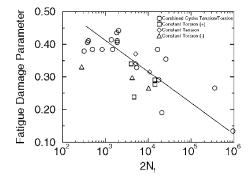

FIG. 12—*Strain damage parameter (Eq 29) versus fatigue life for various multi-axial fatigue experiments.*

of failure. The proposed failure criterion has an excellent correlation with the experimental data. Several multi-axial fatigue failure models were proposed considering the mean and cyclic stresses at the plane of failure, the mean and cyclic strains at the plane of failure, and the mean and cyclic energy. The experimental data had a good correlation with the proposed multi-axial fatigue failure models based on stress and strain at the plane of failure for various tension/torsion experiments. The proposed energy damage model for multi-axial fatigue failure did not correlate well with the experimental data compared to other proposed models. The current work addresses some of the key challenges in studying the fatigue characteristics of fiber-reinforced composites, and, in general, anisotropic materials under multi-axial loading, while emphasizing the need for further systematic studies.

References

[1] Kaynak, C. and Mat, O., "Uniaxial Fatigue Behavior of Filament-Wound Glass/Epoxy Composite Tubes," *Compos. Sci. Technol.*, Vol. 61, 2001, pp. 1833–1840.

[2] Krempl, E. and Niu, T., "Graphite/Epoxy $[\pm 45]_S$ Tubes. Their Static Axial and Shear Properties and Their Fatigue Behavior Under Completely Reversed Load Controlled Loading," *J. Compos. Mater.*, Vol. 16, 1982, pp. 172–187.

[3] Jelf, P. M. and Fleck, N. A., "The Failure of Composite Tubes Due to Combined Compression and Torsion," *J. Mater. Sci.*, Vol. 29, 1994, pp. 3080–3084.

[4] Radon, J. C. and Wachnicki, C. R., "Biaxial Fatigue of Glass Fiber Reinforced Polyester Resin," *Multiaxial Fatigue, ASTM STP 853*, K. J. Miller and M. W. Brown, Eds., ASTM International, West Conshohocken, PA, 1985, pp. 396–412.

[5] Leese, G. E. and Morrow, J., "Low Cycle Fatigue Properties of a 1045 Steel in Torsion," *Multiaxial Fatigue, ASTM STP 853*, K. J. Miller and M. W. Brown, Eds., ASTM International, West Conshohocken, PA, 1985, pp. 482–496.

[6] Fash, J. W., Socie, D. F., and McDowell, D. L., "Fatigue Life Estimates for a Simple Notched Component Under Biaxial Loading," *Multiaxial Fatigue, ASTM STP 853*, K. J. Miller and M. W. Brown, Eds., ASTM International, West Conshohocken, PA, 1985, pp. 497–513.

[7] Ellyin, F. and Golos, K., "Multiaxial Fatigue Damage Criterion," *J. Eng. Mater. Technol.*, Vol. 110, 1988, pp. 63–68.

[8] Ellyin, F., "Effect of Tensile-Mean-Strain on Plastic Strain Energy and Cyclic Response," *J. Eng. Mater. Technol.*, Vol. 107, 1985, pp. 119–125.

[9] Ellyin, F., Golos, K., and Xia, Z., "In-Phase and Out-of-Phase Multiaxial Fatigue," *J. Eng. Mater. Technol.*, Vol. 113, 1991, pp. 112–118.

[10] Ellyin, F. and Xia, Z., "Non-proportional Multiaxial Cyclic Loading: Experiments and Constitute Modeling," *J. Appl. Mech.*, Vol. 58, 1991, pp. 317–325.

[11] Ellyin, F. and Golos, K., "A Total Strain Energy Density Theory for Cumulative Fatigue Damage," *J. Pressure Vessel Technol.*, Vol. 110, 1988, pp. 36–41.

[12] Ellyin, F. and Xia, Z., "A General Fatigue Theory and Its Application to Out-of-Phase Cyclic Loading," *J. Eng. Mater. Technol.*, Vol. 115, 1993, pp. 411–416.

[13] Ellyin, F. and Kujawski, D., "Multiaxial Fatigue Criterion Including Mean-Stress Effect," *Advances in Multiaxial Fatigue, ASTM STP 1191*, D. L. McDowell and R. Ellis, Eds., ASTM International, West Conshohocken, PA, 1993, pp. 55–66.

[14] Lin, H., "Multiaxial Plasticity and Fatigue Life Prediction of Anisotropic Al-6061-T6," Ph.D. Thesis, Northeastern University, Boston, MA, 1993.

[15] Socie, D. F., Waill, L. A., and Dittmer, D. F., "Biaxial Fatigue of Inconel 718 Including Mean Stress Effects," *Multiaxial Fatigue, ASTM STP 853*, K. J. Miller and M. W. Brown, Eds., ASTM International, West Conshohocken, PA, 1985, pp. 463–481.

[16] Stephens, S. I., Fatemi, A., Stephens, R. R., and Fuchs, H. O., *Metal Fatigue in Engineering*, 2nd ed., John Wiley and Sons, Inc., New York, 2001, pp. 331–333.

[17] Bannantine, J. A., Comer, J. J., and Handrock, J. L., *Fundamentals of Metal Fatigue Analysis*, Prentice Hall, Inc., Englewood Cliffs, NJ, 1990, pp. 69–70.

[18] Richardson, D., McLennan, M., Anderson, G., Macon, D., and Batista-Rodriguez, A.,

"Multiaxial Temperature- and Time-Dependent Failure Model," NASA Tech. Briefs, 2003. http:www.nasatech.com/Briefs/Oct03/MFS3175.html

[19] Found, M. S., "A Review of the Multiaxial Fatigue Testing of Fiber Reinforced Plastics," *Multiaxial Fatigue, ASTM STP 853*, K. J. Miller and M. W. Brown, Eds., ASTM International, West Conshohocken, PA, 1985, pp. 318–395.

[20] Caprino, G., "Predicting Fatigue Life of Composite Laminates Subjected to Tension-Tension Fatigue," *J. Compos. Mater.*, Vol. 34, 2000, pp. 1334–1355.

[21] Lin, H., Nayeb-Hashemi, H., Pelloux, R. M. N., and Berg, C. A., "Cyclic Deformation and Anisotropic Constitutive Relations of Al-6061-T6 Under Biaxial Loading," *J. Eng. Mater. Technol.*, Vol. 114, 1992, pp. 323–330.

[22] Lin, H., Nayeb-Hashemi, H., and Pelloux, R. M. N., "Constitutive Relations and Fatigue Life Prediction for Anisotropic Al-6061-T6 Rods Under Biaxial Proportional Loadings," *Int. J. Fatigue*, 14, No. 4, 1992, pp. 249–259.

[23] Van Paepegem, W. and Degrieck, J., "Coupled Residual Stiffness and Strength Model for Fatigue of Fiber-reinforced Composite Material," *Compos. Sci. Technol.*, Vol. 62, No. 5, 2002, pp. 687–696.

[24] Van Paepegem, W. and Degrieck, J., "A New Coupled Approach of Residual Stiffness and Strength for Fatigue of Fiber-reinforced Composites," *Int. J. Fatigue*, Vol. 24, 2002, pp. 747–762.

[25] Van Paepegem, W. and Degrieck, J., "Tensile and Compressive Damage Coupling for Fully-reversible Bending Fatigue of Fiber-reinforced Composites," Fatigue and Fracture of Engineering Materials and Structures, Vol. 25, No. 6, 2002, pp. 547–561.

[26] Degrieck, J. and Van Paepegem, W., "Fatigue Damage Modeling of Fiber-reinforced Composite Materials: Review," *Appl. Mech. Rev.*, Vol. 54, No. 4, 2001, pp. 279–300.

[27] Van Paepegem, W., Degrieck, J., and De Baets, P., "Finite Element Approach for Modeling Fatigue Damage in Fiber-reinforced Composite Materials," *Composites, Part B*, Vol. 32, No. 7, 2001, pp. 575–588.

[28] Shokrieh, M. M. and Taheri-Behrooz, F. T., "A Unified Fatigue Life Model Based on Energy Method," Composite Structures, Thirteenth International Conference on Composite Structures - ICCS/13, Vol. 75, Issues 1–4, 2006, pp. 440–450.

[29] Natarajan, V., Gangarao, H. V. S., and Shekar, V., "Fatigue Response of Fabric-reinforced Polymeric Composites," *J. Compos. Mater.*, Vol. 39, 2005, pp. 1541–1559.

[30] Nayeb-Hashemi, H., Cohen, M. D., Zotos, J., and Poormand, R., "Ultrasonic Characteristics of Graphite/Epoxy Composite Material Subject to Fatigue and Impacts," *J. Nondestruct. Eval.*, Vol. 5, 1986, pp. 119–131.